

Cyclometalated cinchophen ligands on iridium(III): towards water-soluble complexes with visible luminescence†

Rebecca A. Smith, Emily C. Stokes, Emily E. Langdon-Jones, James A. Platts, Benson M. Kariuki, Andrew J. Hallett* and Simon J. A. Pope*

Cite this: *Dalton Trans.*, 2013, **42**, 10347

Received 26th April 2013,
Accepted 29th May 2013

DOI: 10.1039/c3dt51098k

www.rsc.org/dalton

Eight cationic heteroleptic iridium(III) complexes, $[\text{Ir}(\text{epqc})_2(\text{N}^{\wedge}\text{N})]^+$, were prepared in high yield from a cyclometalated iridium bridged-chloride dimer bearing two ethyl-2-phenylquinoline-4-carboxylate (epqc) ligands. Two X-ray crystallographic studies were undertaken on selected complexes (where the ancillary ligand $\text{N}^{\wedge}\text{N}$ = 4,4'-dimethyl-2,2'-bipyridine and 4,7-diphenyl-1,10-phenanthroline) each confirming the proposed formulations, showing an octahedral coordination at Ir(III). In general, the complexes are luminescent (620–630 nm) with moderately long lifetimes indicative of phosphorescence. Hydrolysis of the ethyl ester moieties of the epqc ligands gave the analogous cinchophen-based complexes, which were water-soluble and visibly luminescent (568–631 nm). The spectroscopic and redox characterisation of the complexes was complemented by DFT and TD-DFT calculations, supporting the assignment of dominant $^3\text{MLCT}$ to the emissive character.

Introduction

There has been considerable attention and effort disbursed on iridium(III) complexes with cyclometalated ligands, due to their tuneable and generally efficient photoluminescence properties and subsequent performance in a variety of photo-physical and electronic applications.¹ Such complexes are capable of showing intense phosphorescence at room temperature;² the heavy atom iridium centre mediating strong spin-orbit coupling and intersystem crossing (ISC), mixing the singlet and triplet excited states and generating high phosphorescent efficiencies. As a consequence, cyclometalated iridium complexes have found many applications in a variety of opto-electronically related applications, such as electrochemical cells,³ photovoltaics,⁴ and luminescence imaging.⁵ Their ability to perform in such roles relies upon an understanding of their excited state properties, which can be modulated by altering the cyclometalating and/or ancillary ligand associated with the iridium centre. The ability to tune

luminescence emission wavelengths through variation of cyclometalating ligands and ancillary ligands (predominantly for cationic complexes) renders such complexes very useful, particularly in electrochemiluminescence (ECL).⁶ For example, increasing the π -conjugation of phenylpyridine by adding an aromatic ring (to give phenylquinoline) bathochromically shifts the $^3\pi\text{-}\pi^*$ and triplet metal-to-ligand charge transfer ($^3\text{MLCT}$) emission due to lower lying π^* orbitals.⁷ Consequently, there have been several reports of phenylquinoline derivatives as cyclometalating ligands with various ancillary ligands.⁸ However, many applications of Ir(III) complexes in this context, including biologically-related uses, require water solubility. Surprisingly then, there have only been a handful of reports of water-soluble iridium cyclometalated complexes, most commonly where the ancillary diimine ligands are functionalised with solubilising groups such as sugars,^{8j,l} triazoles,⁹ polyethyleneglycol (PEG),¹⁰ bioconjugates¹¹ and carboxylate groups,¹² as well as the bis-cyclometalated bis-aqua complexes;¹³ reports of water-solubilising functionalisation at the cyclometalating ligand are extremely rare.¹⁴ The purpose of this paper is to present the synthesis and photo-physical properties of a class of iridium complex that incorporate cyclometalated cinchophen-based ligands, providing a convenient route towards water-soluble complexes with exploitable photophysical properties; the structural, spectroscopic, electrochemical and photophysical studies are presented together with supporting DFT and TD-DFT calculations on the complexes.

School of Chemistry, Main Building, Cardiff University, Cardiff CF10 3AT, UK.
E-mail: popesj@cardiff.ac.uk, hallettaj@cardiff.ac.uk; Fax: +44 (0) 29-20874030;
Tel: +44 (0) 29-20879316

†Electronic supplementary information (ESI) available: Data collection parameters for the crystallographic studies, electrochemical data for **3a–h**, pictorial representations of the calculated frontier orbitals for **3a–h** and **4a–h** and Cartesian coordinates obtained from DFT calculations. CCDC 907280 and 907282. For ESI and crystallographic data in CIF or other electronic format see DOI: 10.1039/c3dt51098k



Results and discussion

Synthesis and characterisation of the ligands and complexes

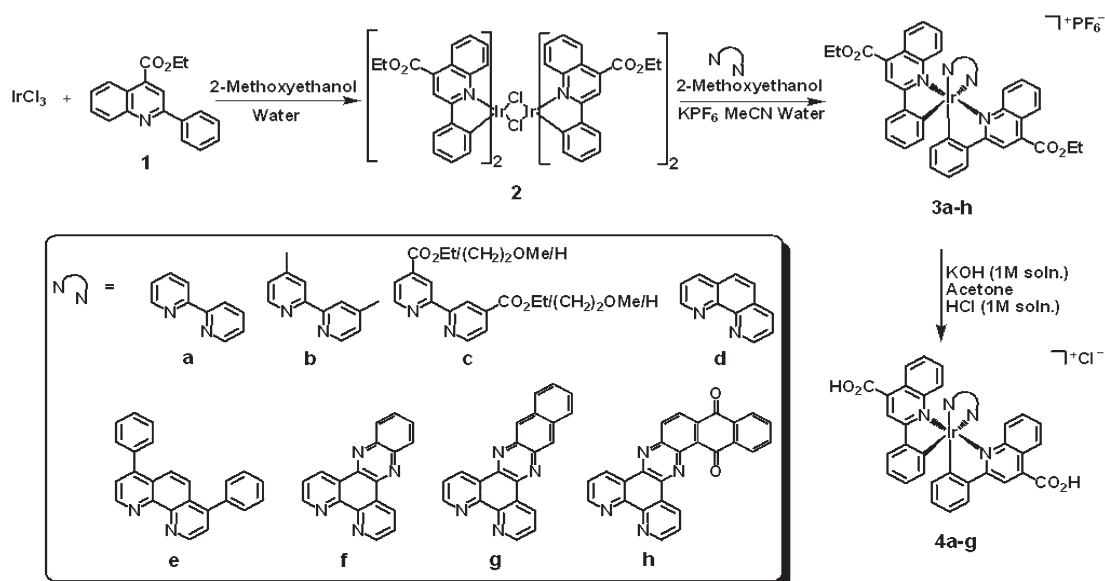
As an aside, it is noteworthy that many of the literature reports on functionalised phenylquinoline compounds describe biological activities¹⁵ with applications as anti-malarial, anti-inflammatory and antibacterial agents;¹⁶ ester-functionalised phenylquinoline compounds have shown promise as amyloid fibril¹⁷ and reverse transcriptase¹⁸ inhibitors. Ethyl-2-phenylquinoline-4-carboxylate (epqcH) was prepared by simply dissolving and heating 2-phenylquinoline-4-carboxylic acid (cinchophen) in ethanol with a few drops of conc. H₂SO₄. The precursor iridium chloro-bridged dimer [(epqc)₂Ir(μ-Cl)₂Ir(epqc)₂] (2) was synthesised according to established literature conditions.¹⁹ Compound 2 readily reacted (Scheme 1) with a range of selected diimine-type ligands in 2-methoxyethanol; work-up and counter anion exchange yielded the crude monometallic complexes, [Ir(epqc)₂(N[^]N)]PF₆ {N[^]N = 2,2'-bipyridine (bpy) **3a**; 4,4'-dimethyl-2,2'-bipyridine (dmbpy) **3b**; 1,10-phenanthroline (phen) **3d**; 4,7-diphenyl-1,10-phenanthroline (dip) **3e**; dipyrdo[3,2-*a*:2',3'-*c*]phenazine (dppz) **3f**; benzo[*f*]dipyrido[3,2-*a*:2',3'-*c*]phenazine (dppn) **3g**; naphtha[2,3-*a*]dipyrido[3,2-*h*:2',3'-*f*]phenazine-5,18-dione (qdppz) **3h**}. For the reaction of 2 and diethyl-2,2'-bipyridine-4,4'-dicarboxylate (debpy), the ethyl ester groups of bpy were selectively converted to 2-methoxyethyl esters *in situ*, as informed by ¹H NMR spectroscopy and mass spectrometry therefore giving [Ir(epqc)₂(dmbpc)]PF₆ **3c** (dmbpc = di-2-methoxyethyl-2,2'-bipyridine-4,4'-dicarboxylate). It should be noted that the ethyl ester functionality of the cyclometalated cinchophen ligand was retained in all cases. Further purification for each complex was achieved using column chromatography (silica; MeOH-CH₂Cl₂, 1:9) with elution of the first red band and subsequent removal of solvent giving the complexes as pure red-coloured powders in

good yields (>75%). The resultant complexes **3a-h** were soluble in a range of common organic solvents.

The conversion of complexes **3a-g** to their corresponding free acids was achieved by stirring the esterified complexes in an equi-volume mixture of 1 M KOH and acetone under an inert atmosphere. Subsequent neutralisation with 1 M HCl, removal of solvent and extraction with methanol (allowing removal of KCl) led to the isolation of complexes **4a-g** as their chloride salts, [Ir(pqca)₂(N[^]N)]Cl. However, ¹H NMR spectroscopy and mass spectrometry indicated that it was not possible to isolate **4h** by this method, the reasons for which are currently unknown.

All new complexes were characterised using a range of spectroscopic techniques. Firstly, the ¹H NMR spectra of complexes **3a-h** are complicated in the aromatic region with overlapping resonances associated with the cyclometalated and diimine ligands; the retention of the ethyl ester functionality was observed in the aliphatic region. The 2-methoxyethyl groups of **3c** appeared as broadened triplets at 4.46 and 3.68 ppm together with a singlet at 3.30 ppm. ³¹P-{¹H} NMR spectroscopy confirmed the presence of the PF₆⁻ ion with a signature septet (¹J_{PF}) at *ca.* -145 ppm in all cases. Low and high resolution mass spectra were obtained for the complexes **3a-h** and each confirmed the identity of the cationic, monomeric species of type [(epqc)₂Ir(N[^]N)]⁺, revealing the parent cations of [M - PF₆]⁺ in each case, with the appropriate isotopic distribution. Complex purity was confirmed by elemental analysis.

Upon hydrolysis of the ester groups, the ¹H NMR spectra of the isolated analogues **4a-g** all confirmed the absence of the ethyl, or 2-methoxyethyl groups in the case of **4c**, yielding 2,2'-bipyridyl-4,4'-dicarboxylic acid (bpdc), as well as improved resolution of the aromatic resonances. The absence of a resonance in the ³¹P-{¹H} NMR spectra indicated the exchange of PF₆⁻ with Cl⁻ counter ions in the deprotected species. The



Scheme 1 Synthetic route to complexes [Ir(epqc)₂(N[^]N)]PF₆ **3a-h** and [Ir(pqca)₂(N[^]N)]Cl **4a-g**.



corresponding mass spectra were easily obtained: complexes **4a–g** confirmed the identity of the cationic, monomeric species of type $[\text{Ir}(\text{pqca})_2(\text{N}^{\wedge}\text{N})]^+$ showing the characteristic cluster of peaks associated with the $[\text{M} - \text{Cl}]^+$ parent ion. Solid-state IR spectra were also obtained on all complexes highlighting the conversion from ester (*ca.* 1720 cm^{-1}) to carboxylate (*ca.* 1580 cm^{-1}) *via* significant low energy shifts in $\nu(\text{C}=\text{O})$, and the absence of the PF_6^- counter ion stretch (*ca.* 835 cm^{-1}) confirming exchange with chloride.

X-ray crystallography studies

Single crystals of **3b** and **3e** suitable for X-ray diffraction studies were isolated following vapour diffusion of Et_2O into concentrated CHCl_3 or MeCN solutions of the complexes, over a period of 48 h at $-20\text{ }^\circ\text{C}$. The bond lengths and bond angles are reported in Table 1, and the associated data collection parameters are reported in Table S1, ESI.†

The structures obtained for the three complexes (Fig. 1a and 2a) confirmed the proposed formulations, and show that the iridium(III) center in these $[\text{Ir}(\text{epqc})_2(\text{N}^{\wedge}\text{N})]^+$ complexes adopts a distorted octahedral coordination geometry. *trans* Angles at the metal centers ranged from $168.0(3)^\circ$ to $172.4(3)^\circ$ for **3b** and $168.0(3)^\circ$ to $174.9(3)^\circ$ for **3e**. The diimine ligand is always coordinated *trans* to the cyclometalated phenyl rings; the complexes retain the *cis*-C,C and *trans*-N,N chelating disposition of the original chloro-bridged dimer as reported in related examples.^{7c,20} The *trans*-influence of the carbon donors rendered slightly longer Ir–N bond lengths for the diimine ligands {2.182(8) and 2.158(7) Å for **3b**} than the epqc ligands {2.094(8) and 2.112(8) Å for **3b**}. The bite angles of the epqc ligands ($80.0(4)^\circ$ and $80.3(4)^\circ$ for **3b**) were slightly larger than that of $\text{N}^{\wedge}\text{N}$ ligands { $75.1(3)$ for **3b**}. Similar observations have been reported in related cyclometalated iridium(III) polypyridine systems $[\text{Ir}(\text{pq})_2(\text{N}^{\wedge}\text{N})]^+$.^{1e,7c,d,20} For **3e** the structure showed that the phenyl substituents of the 4,7-diphenyl-1,10-phenanthroline ligand are twisted out of planarity from the phenanthroline unit by 55.1° and 50.2° respectively. In addition, as with related phenylquinoxaline complexes,^{7d,21} there is a distortion within the quinoline moiety caused by the

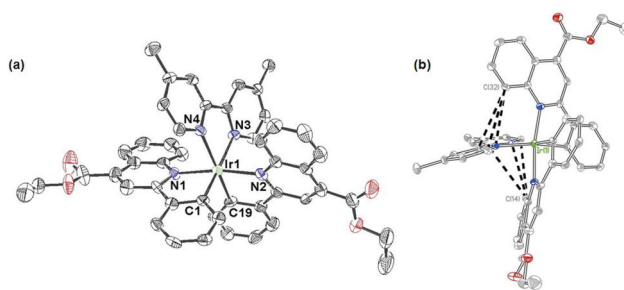


Fig. 1 (a) Ortep representation of $[\text{Ir}(\text{epqc})_2(\text{dmbpy})]^+$ **3b** (50% probability ellipsoids, solvent molecules, PF_6^- anion and hydrogen atoms have been omitted for clarity) and (b) showing non-bonding contact interactions between chelating ligands.

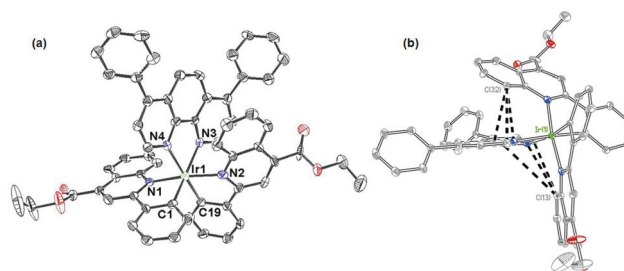


Fig. 2 (a) Ortep representation of $[\text{Ir}(\text{epqc})_2(\text{dip})]^+$ **3e** (50% probability ellipsoids, solvent molecules, PF_6^- anion and hydrogen atoms have been omitted for clarity) and (b) showing non-bonding contact interactions between chelating ligands.

steric interactions between the chelating ligands (Fig. 1b and 2b). Some of the inter-ligand $\text{C}\cdots\text{C}$ and $\text{C}\cdots\text{N}$ non-bonding contact distances (Table 1) are shorter than 3.4 \AA (*i.e.* the sum of the van der Waals radii of the atoms). This results in the phenyl groups of the epqc ligand showing deformation angles of 14.1° and 19.1° for **3b** and 17.5° and 28.6° for **3e** with respect to the quinoline fragment of the ligand.

The bond lengths and angles of **3b** and **3e** were compared with the optimised values calculated from density functional theory (DFT) studies (also see DFT section and Table 1). In general, a reasonable agreement was obtained between the theoretical and experimentally observed bond lengths, although some small differences were found. The calculated $\text{Ir}-\text{N}_{\text{bipyridine}}$ bond lengths, $\text{Ir}-\text{N}(3)$ and $\text{Ir}-\text{N}(4)$, are 0.038 and 0.062 \AA longer than the experimental values for **3b**. In the case of the cyclometalated Ir–C bonds, calculated values are very similar to the experimentally obtained data for $\text{Ir}-\text{C}(1)$ in **3b** and **3e**; similarly the $\text{Ir}-\text{N}_{\text{quinoline}}$ bonds, where the calculated and experimental values are comparable. Again, the calculated structures reveal $\text{C}\cdots\text{C}$ and $\text{C}\cdots\text{N}$ interactions between the ligands. The calculated deformation angles of the quinoline fragment are much lower for **3b** and **3e**.

Density functional theory (DFT) studies

DFT calculations (computed using the B3PW91 hybrid functional) were performed to investigate the frontier orbitals and provide qualitative descriptions of the highest occupied

Table 1 Selected bond lengths (Å) and angles ($^\circ$) for complexes **3b** and **3e**

Bond length (Å)/ angle ($^\circ$)	3b	Calculated value	3e	Calculated value
$\text{Ir}(1)-\text{N}(1)$	2.094(8)	2.107	2.078(6)	2.107
$\text{Ir}(1)-\text{N}(2)$	2.112(8)	2.107	2.107(7)	2.107
$\text{Ir}(1)-\text{N}(3)$	2.182(8)	2.220	2.190(6)	2.218
$\text{Ir}(1)-\text{N}(4)$	2.158(7)	2.220	2.153(7)	2.218
$\text{Ir}(1)-\text{C}(1)$	1.998(9)	1.997	1.989(8)	1.997
$\text{Ir}(1)-\text{C}(19)$	2.001(9)	1.997	2.005(8)	1.997
$\text{C}(14)\cdots\text{N}(3)$	3.140 ^a	3.127	3.009 ^a	3.128
$\text{C}(32)\cdots\text{N}(4)$	3.173 ^a	3.128	3.232 ^a	3.128
$\text{N}(1)-\text{Ir}(1)-\text{N}(2)$	170.7(3)	172.1	173.3(3)	172.8
$\text{N}(1)-\text{Ir}(1)-\text{C}(1)$	80.0(4)	80.0	79.4(5)	79.9
$\text{N}(2)-\text{Ir}(1)-\text{C}(19)$	80.3(3)	80.0	79.9(3)	79.9
$\text{C}(1)-\text{Ir}(1)-\text{C}(19)$	89.2(4)	90.1	88.6(3)	90.5

^a Non-bonded metrics and those involving planes/centroids were not included in the refinement, and thus do not have an e.s.d.



molecular orbital (HOMO) and lowest unoccupied molecular orbital (LUMO) energy levels.

For the $[\text{Ir}(\text{epqc})_2(\text{N}^{\wedge}\text{N})]^+$ complexes, the energy levels of the HOMO are sufficiently different ($\Delta E > 0.2$ eV) from the other MOs to be considered independent. In each case the HOMO was located on the metal 5d(Ir) centre and cyclometalated phenyl rings (Fig. S1, ESI[†]), with little or no coverage of the ancillary diimine ligands. However, varying the diimine ligands does impart a subtle perturbation of the HOMO energy ($E_{\text{HOMO}} = -7.66$ to -7.84 eV). The LUMO for the complexes is, in many cases, close enough in energy to be considered isoenergetic with other close-lying MOs (e.g. LUMO + 1, LUMO + 2). For the complexes where this is not the case (**3c**, **3f**, **3g** and **3h**), the LUMOs are predominantly delocalised over the diimine ligands as with previous studies of related compounds.^{7d} For **3a**, **3b**, **3d** and **3e** the orbitals show a mixture of diimine and phenylquinoline localisation. The diimine imparts a larger degree of variation in the energy levels of the LUMO energy ($E_{\text{LUMO}} = -4.71$ to -5.47 eV), with **3h** showing the lowest LUMO energy level ($E_{\text{LUMO}} = -5.47$ eV) and, therefore, smallest bandgap ($E_{\text{bandgap}} = 2.29$ eV). These results suggest that the lowest energy absorption is predicted to comprise of significant MLCT character and that variation of the diimine ligand could lead to a small degree of tuneable optical properties within this series of complexes. The corresponding cinchophen complexes (**4a–h**) showed the same general localisation of the frontier orbitals, but revealed a drop in both the HOMO and LUMO energies by an average of 0.12 eV and 0.13 eV, respectively (Fig. S2, ESI[†]).

Electrochemical studies

The electrochemical characteristics of the $[\text{Ir}(\text{epqc})_2(\text{N}^{\wedge}\text{N})]\text{PF}_6$ (**3a–h**) complexes were studied in de-oxygenated CH_2Cl_2 . The HOMO energy levels (E_{HOMO}) were determined from the ionisation potential of the first oxidation ($\text{Ir}^{3+/4+}$) by direct correlation with the redox couple of $\text{FeCp}_2^{0/1+}$. The cyclic voltammograms, measured at a platinum disc electrode (scan rate $\nu = 200$ mV s^{-1} , 1×10^{-3} M solutions, 0.1 M $[\text{NBu}_4][\text{PF}_6]$ as a supporting electrolyte), each showed one non-fully reversible oxidation (Table S2, ESI[†]), over the range +1.38 to +1.45 V. The extent of the irreversibility can be ascribed to the contribution of the cyclometalating ligands to the electron density of the HOMO,²² which in this case is calculated to be ca. 45% from DFT studies. The E_{HOMO} values were determined using the relevant equations²³ and the resultant values fall in the narrow range -5.72 to -5.83 eV (Table S3, ESI[†]). Each complex also showed one or two partially reversible or irreversible reduction waves, assigned to ligand-centred processes involving both the diimine and phenylquinoline ligands, with complex **3h** showing at least four reduction processes, some of which must be associated with the highly reducible anthraquinone fragment.

Electronic properties of the complexes

The UV-vis absorption spectra of complexes **3a–h** were obtained as aerated MeCN solutions (5×10^{-5} M) (Fig. 3,

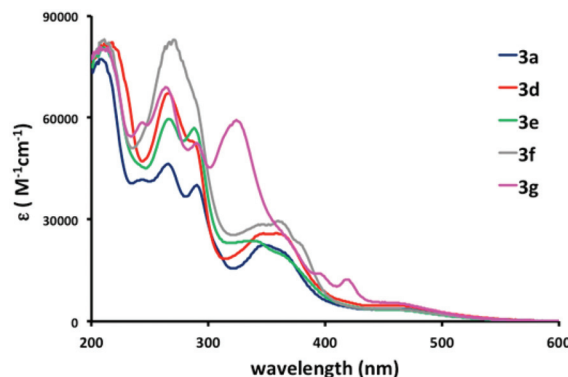


Fig. 3 UV-vis spectra of selected $[\text{Ir}(\text{epqc})_2(\text{N}^{\wedge}\text{N})]\text{PF}_6$ complexes in MeCN solutions (5×10^{-5} M).

Table 3). Strong absorption bands between 250 and 380 nm were assigned to spin allowed $^1\pi\text{-}\pi^*$ ligand-centered (LC) transitions arising from both the cyclometalated and diimine ligands within each complex. Weaker bands at 380–480 nm in the visible region were assigned to spin-allowed metal-to-ligand charge transfer bands ($^1\text{MLCT}$) with the possibility of spin-forbidden $^3\text{MLCT}$ transitions contributing to the weaker low-energy shoulder. For **3h** it is also likely that ligand-centred transitions associated with the anthraquinone moiety also contribute in this wavelength region; previous studies have shown that such species can possess intra-ligand CT (formally $n\text{-}\pi^*$) character, which is likely to contribute to the lower energy parts of the spectral profile. The variation in coordinated diimine ligand imparts only a very minor variation in the wavelength positioning of the visible absorption bands. As expected the absorption spectra of the corresponding carboxylic acid derivatives **4a–g** (5×10^{-5} M MeOH) share many of the same common features. The principal observation from these spectra is that the visible MLCT-based bands appear as a defined transition ca. 430–455 nm.

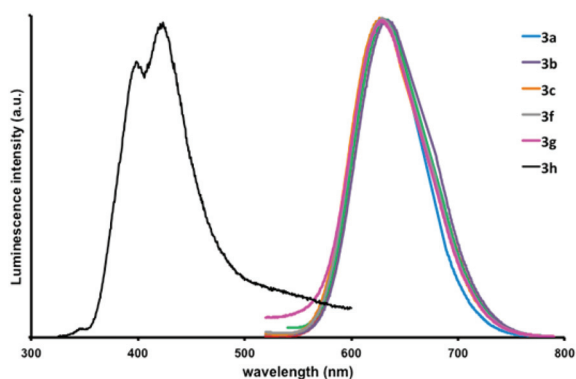
TD-DFT calculations (Table 2) in simulated MeCN suggest the assignment of the lowest lying absorption bands as having substantial MLCT character. For **3a** the lowest energy absorption involves excitation from HOMO (Ir-5d + phenyl- π) to LUMO + 1 (quinoline- π^*), predicted to lie at 528 nm (oscillator strength = 0.04 au), and so coincides reasonably closely with the lowest energy shoulder feature seen in Fig. 4. A set of stronger bands centred around 370 nm (387 nm, 0.15 au; 375 nm, 0.17 au; 359 nm, 0.10 au) is also predicted, again in good agreement with Fig. 4. These bands consist of varying combinations of Ir-5d and epqc- π orbitals excited into epqc- π^* orbitals, but have no contribution from the ancillary bpy- π^* orbitals. In comparison, TD-DFT simulation of **3c** in MeCN results in broadly the same pattern of predicted bands at 520 nm (0.04 au), 406 nm (0.06 au), 389 nm (0.07 au) and 384 nm (0.09 au), although the higher energy bands are reduced in intensity relative to the low energy MLCT band. In this complex, two low energy bands involving excitation from HOMO (Ir 5d + phenyl- π) to LUMO and LUMO + 1 (bipy- π^* and quinoline- π^* , respectively) are predicted at 564 and 522 nm,



Table 2 Calculated excitation wavelengths for **3a** and **4a** from TD-DFT studies showing the dominant transitions

3a (ester)			4a (acid)			4a (carboxylate)		
λ^a (nm)	f^b	Character	λ (nm)	f	Character	λ (nm)	f	Character
528	0.0422	HOMO \rightarrow LUMO + 1	543	0.0348	HOMO \rightarrow LUMO + 1	456	0.056	HOMO \rightarrow LUMO
411	0.0538	HOMO - 1 \rightarrow LUMO	420	0.0509	HOMO - 1 \rightarrow LUMO	406	0.021	HOMO - 3 \rightarrow LUMO
387	0.1495	HOMO - 2 \rightarrow LUMO + 1	394	0.1245	HOMO - 2 \rightarrow LUMO + 1	381	0.056	HOMO - 3 \rightarrow LUMO + 1
385	0.0469	HOMO - 2 \rightarrow LUMO	392	0.0421	HOMO - 2 \rightarrow LUMO	366	0.115	HOMO - 6 \rightarrow LUMO + 2
375	0.1743	HOMO - 3 \rightarrow LUMO	383	0.1547	HOMO - 3 \rightarrow LUMO	363	0.060	HOMO - 3 \rightarrow LUMO + 3
359	0.1040	HOMO - 4 \rightarrow LUMO	366	0.1732	HOMO - 4 \rightarrow LUMO + 1	356	0.045	HOMO - 7 \rightarrow LUMO + 1
		HOMO - 4 \rightarrow LUMO + 1						
359	0.0815	HOMO - 4 \rightarrow LUMO	364	0.0478	HOMO - 4 \rightarrow LUMO	355	0.037	HOMO - 7 \rightarrow LUMO + 2
		HOMO - 4 \rightarrow LUMO + 1			HOMO - 1 \rightarrow LUMO + 2			

^a Excitation wavelength. ^b Oscillator strength.

**Fig. 4** Normalised luminescence emission spectra of selected $[\text{Ir}(\text{epqc})_2(\text{N}^{\wedge}\text{N})]\text{-PF}_6$ complexes in MeCN solutions (5×10^{-5} M).

but with very low intensity (<0.001 au), suggesting the possibility of MLCT/LLCT character.

Deprotection of the ester to yield complex **4a** was modelled using both the neutral acid and deprotonated carboxylate form. In the neutral complex, calculations predict a red-shift of the absorption bands discussed above by *ca.* 15 nm, and alteration of the relative intensities of the absorptions, with predicted bands lying at 544 nm (oscillator strength of 0.04 au), 394 nm (0.12 au), 383 nm (0.15 au) and 365 nm (0.18 au). In contrast, simulation of the deprotonated carboxylate form of **4a** indicates a substantial blue-shift of the absorption bands, with the lowest energy absorption with significant oscillator strength coming at 456 nm (0.6 au), and a more intense band at 365 nm (0.12 au). The latter approach is in much better agreement with the experimental data, such that modelling **4a** as the bis-carboxylate form seems to be more appropriate.

Steady state luminescence measurements were conducted on aerated MeCN solutions, irradiating the ¹MLCT wavelength ($\lambda_{\text{ex}} = 450$ nm) absorption (Table 3, Fig. 4). The emission maxima for complexes **3a–g** show very little variation (627–630 nm), are broad and featureless, and typically characteristic of MLCT-based transitions.²⁴ This variation is less than that predicted by TD-DFT (see ESI[†]), possibly suggesting a diminished diimine contribution to the excited state. Corresponding excitation spectra showed that the complexes could

Table 3 Photophysical properties of $[\text{Ir}(\text{epqc})_2(\text{N}^{\wedge}\text{N})]\text{PF}_6$ (**3a–h**) complexes^a

Complex	λ_{abs}^a (nm)	λ_{em}^a (nm)	$\tau^{a,b}$ (ns)	Φ^a
3a	470 (4500), 350 (22 000), 292 (39 500), 268 (45 650)	627	219	0.022
3b	467 (4200), 350 (23 500), 290 (46 500), 265 (55 300)	630	211	0.020
3c	464 (2850), 352 (18 150), 291 (39 500), 267 (47 850)	620	189	0.020
3d	460 (4500), 356 (25 750), 288 (52 750), 269 (65 350)	630	178	0.029
3e	465 (3550), 344 (23 300), 290 (55 950), 269 (59 000)	628	181	0.019
3f	463 (3650), 364 (29 700), 272 (82 550)	628	210	0.019
3g	461 (5450), 416 (12 100), 398 (13 550), 327 (58 600), 292 (51 900), 266 (68 200)	628	173	0.018
3h	460 (4550), 367 (29 500), 278 (83 750)	426	2.1 (57%), <1 (43%)	— ^c

^a MeCN solution. ^b $\lambda_{\text{ex}} = 459$ nm. ^c Not measured.

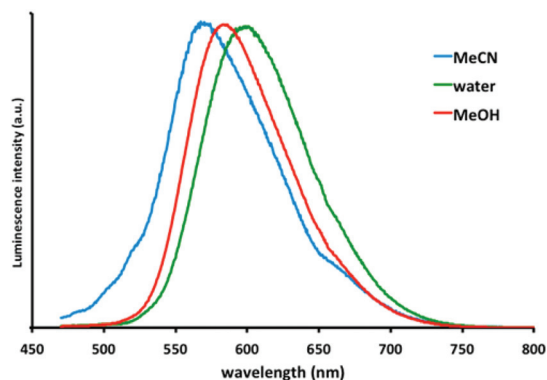
be excited up to a wavelength of *ca.* 520 nm. Time-resolved emission lifetime measurements revealed that the decays were single-exponential, in each case *ca.* 200 ns, typical of ³MLCT character. The complexes each exhibited modest quantum yields (Φ) in aerated MeCN, in line with related species. For **3h**, the emission profile was very different, with a higher energy peak at 422 nm ($\tau < 5$ ns), which was assigned to a ligand-centred transition arising from the anthraquinone chromophore, with no evidence of a comparable MLCT transition. The absence of ³MLCT emission is attributed to the quenching of that state by the anthraquinone-based ancillary ligand.

For ease of comparison the corresponding emission and excitation of the deprotected complexes **4a–g** were obtained in MeCN, MeOH and water. With the exception of **4f** these species all showed a hypsochromic shift of *ca.* 50 nm in the ³MLCT emission maxima (Table 4). Similar measurements in water resulted in an emission peak at *ca.* 595 nm, revealing the solvent-sensitivity and dipolar nature of the excited state. Emission wavelengths in methanol were typically intermediate between those for water and acetonitrile (for example, Fig. 5). Relative to the esterified analogues (**3a–g**), the measured



Table 4 Photophysical properties of $[\text{Ir}(\text{pqca})_2(\text{N}^{\wedge}\text{N})]\text{Cl}$ (**4a–g**) complexes^a

Complex	CH_3CN		H_2O		CH_3OH	
	$\lambda_{\text{em}}/\text{nm}$	τ/ns	$\lambda_{\text{em}}/\text{nm}$	τ/ns	$\lambda_{\text{em}}/\text{nm}$	τ/ns
4a	569	211	592	261	583	414
4b	572	320	594	223	586	383
4c	574	258	589	190	582	385
4d	574	439	590	201	584	446
4e	577	322	608	619	585	370
4f	631	174	630	58	630	82
4g	568	113	598	199	584	297

^a $\lambda_{\text{ex}} = 459 \text{ nm}$.**Fig. 5** Normalised luminescence emission spectra of **4g** in various solvents ($5 \times 10^{-5} \text{ M}$).

lifetimes were generally extended for complexes **4a–g** reflecting the increased energy gap. However, in water the lifetime values also varied greatly as a function of the type of diimine ligand, with **4e** (likely to be the most hydrophobic of the diimines in this study) displaying the longest lifetime ($\tau = 619 \text{ ns}$), suggesting greater shielding of the excited state from the surrounding solvent.

The longer emission wavelength of **4f** in all solvents appears somewhat anomalous and could be due to a number of factors. With reference to the TD-DFT calculations, the protonation state of the cinchophen ligands influences the emission wavelength. Repeating the measurement in 0.1 M NaOH blue-shifted the emission peak to *ca.* 590 nm, in accordance with the other complexes in the cinchophen-based series. However, it is difficult to rationalise why only **4f** (*versus* **4g**, for example) would retain a protonated carboxylic acid form. An alternative explanation considers the role of protonation at the dppz ligand. The closely related species $[\text{Ir}(\text{ppy})_2(\text{dppz})]^+{}^{25}$ reveals $\lambda_{\text{em}} = 630 \text{ nm}$ in MeCN and is thus very comparable to **4f**. However, H-bonding interactions with the phenazine nitrogens can dramatically influence the emission properties; in fact, $[\text{Ir}(\text{ppy})_2(\text{dppz})]^+$ is non-emissive in water, unlike **4f**. The reported photophysics of $[\text{Ir}(\text{ppy})_2(\text{dppn})]^+{}^{25}$ also compare very well ($\lambda_{\text{em}} = 583 \text{ nm}$ in MeOH) to **4g**, and thus the differences in emission wavelength for **4f** could be due to protonation interactions at dppz²⁶ (of course, these would also be sensitive to the addition of 0.1 M NaOH).

Experimental section

All reactions were performed with the use of vacuum line and Schlenk techniques. Reagents were commercial grade and used without further purification. ^1H and $^{13}\text{C}\{-^1\text{H}\}$ NMR spectra were recorded on an NMR-FT Bruker 400 or 250 MHz and $^{31}\text{P}\{-^1\text{H}\}$ NMR spectra on a Joel Eclipse 300 MHz spectrometer and recorded in CDCl_3 or MeOD solutions. ^1H and $^{13}\text{C}\{-^1\text{H}\}$ NMR chemical shifts (δ) were determined relative to internal tetramethylsilane, $\text{Si}(\text{CH}_3)_4$ and are given in ppm. Low-resolution mass spectra were obtained by the staff at Cardiff University. High-resolution mass spectra were carried out at the EPSRC National Mass Spectrometry Service at Swansea University, UK. UV-Vis studies were performed on a Jasco V-650 spectrophotometer fitted with a Jasco temperature control unit in MeCN or MeOH solutions ($5 \times 10^{-5} \text{ M}$) at 20 °C. Photophysical data were obtained on a JobinYvon–Horiba Fluorolog spectrometer fitted with a JY TBX picoseconds photodetection module in MeCN, MeOH or H_2O solutions. Emission spectra were uncorrected and excitation spectra were instrument corrected. The pulsed source was a Nano-LED configured for 372 or 459 nm output operating at 500 kHz. Luminescence lifetime profiles were obtained using the JobinYvon–Horiba FluoroHub single photon counting module and the data fits yielded the lifetime values using the provided DAS6 deconvolution software. Electrochemical studies were carried out using a Parstat 2273 potentiostat in conjunction with a three-electrode cell. The auxiliary electrode was a platinum wire and the working electrode a platinum (1.0 mm diameter) disc. The reference was a silver wire separated from the test solution by a fine porosity frit and an agar bridge saturated with KCl. Solutions ($10 \text{ ml CH}_2\text{Cl}_2$) were $1.0 \times 10^{-3} \text{ mol dm}^{-3}$ in the test compound and 0.1 mol dm^{-3} in $[\text{NBu}^n_4][\text{PF}_6]$ as the supporting electrolyte. Under these conditions, E^0 , for the one-electron oxidation of $[\text{Fe}(\eta\text{-C}_5\text{H}_5)_2]$ added to the test solutions as an internal calibrant, is +0.46 V in CH_2Cl_2 .²⁷ Unless specified, all electrochemical values are at $\nu = 200 \text{ mV s}^{-1}$. Microanalyses were performed by London Metropolitan University, UK.

Data collection and processing

Diffraction data for **3b** and **3e** were collected on a Nonius Kappa-CCD using graphite-monochromated Mo-K α radiation ($\lambda = 0.71073 \text{ \AA}$) at 150 K. Software package Apex 2 (v2.1) was used for the data integration, scaling and absorption correction.

Structure analysis and refinement

The structure was solved by direct methods using SHELXS-97 and was completed by iterative cycles of ΔF -syntheses and full-matrix least squares refinement. All non-H atoms were refined anisotropically and difference Fourier syntheses were employed in positioning idealised hydrogen atoms and were allowed to ride on their parent C-atoms. All refinements were against F^2 and used SHELX-97.²⁸ CCDC reference numbers 907280 and 907282 contain the supplementary crystallographic data for this paper.



DFT studies

DFT geometry optimisation and orbital calculations were performed on the Gaussian 03 program.²⁹ Geometry optimisations were carried out without constraints using the B3PW91 functional. The LANL2DZ³⁰ basis set was used for the Ir centers, and was invoked with pseudo-potentials for the core electrons, a 6-31G(d,p)³¹ basis set for all coordinating atoms with a 6-31G³² basis set for all remaining atoms. All optimisations were followed by frequency calculations to ascertain the nature of the stationary point (minimum or saddle point). TD-DFT studies were performed in Gaussian09³³ using the same functional, but with 6-31G(d) on all non-metal atoms, and also included a simulated MeCN or H₂O environment using the polarised continuum model (PCM) approach.³⁴ For prediction of absorption spectra, the geometry used to calculate orbital and other properties was used without modification. For prediction of emission, however, the triplet state was allowed to relax to its optimal geometry using unrestricted B3PW91 in the gas phase, prior to solvated TD-DFT.

Synthesis

The ligands ethyl 2-phenylquinoline-4-carboxylate (epqcH) **1**,³⁵ dipyrido[3,2-*a*:2',3'-*c*]phenazine (dppz),³⁶ benzo[*i*]dipyrido[3,2-*a*:2',3'-*c*]phenazine (dppn)³⁷ and naphtha[2,3-*a*]dipyrido[3,2-*h*:2',3'-*f*]phenazine-5,18-dione (qdppz)³⁸ were prepared according to reported procedures.

[Ir(epqc)₂(μ-Cl)₂Ir(epqc)₂] **2** was prepared by variation of the standard literature procedures for other bridged-chloride dimers.¹⁹ Thus, IrCl₃·3H₂O (0.266 g, 0.75 mmol) and epqcH (0.520 g, 2.02 mmol) in 2-methoxyethanol–water (3 : 1, 8 ml) were heated at reflux for 48 h. Water (25 ml) was added to give a dark purple precipitate, which was filtered and dried *in vacuo*. The product was used in subsequent reaction without further purification.²⁴

[Ir(epqc)₂(bpy)]PF₆ **3a**. **[(epqc)₂Ir(μ-Cl)₂Ir(epqc)₂]** **2** (0.061 g, 0.04 mmol) and 2,2'-bipyridine (0.013 g, 0.08 mmol) in 2-methoxyethanol (5 ml) were heated at 120 °C for 16 h. The solvent was then removed *in vacuo* and the crude product dissolved in MeCN (4 ml). KPF₆ (1.05 g, 5.705 mmol) in water (2 ml) was added and the solution stirred for 10 min. Water (20 ml) was added and the product extracted with CH₂Cl₂ (2 × 20 ml). The combined organic phases were washed with water (30 ml) and brine (30 ml) before being dried over MgSO₄. The solution was filtered and the solvent removed *in vacuo*. The crude product was then purified by column chromatography (silica, CH₂Cl₂). After elution of unreacted organics with CH₂Cl₂ the product was eluted as the first red fraction with CH₂Cl₂–MeOH (9 : 1). The product was concentrated in volume (to *ca.* 3 ml) and precipitated by the slow addition of Et₂O (5 ml) and dried *in vacuo*. Yield = 0.055 g, 76%. ¹H NMR (250 MHz, CDCl₃) δ_H = 8.51 (2H, s), 8.42 (2H, d, ³J_{HH} = 5.8 Hz), 8.23 (2H, d, ³J_{HH} = 7.5 Hz), 8.05–7.8 (6H, m), 7.70–7.35 (6H, m), 7.21 (2H, app. t, ³J_{HH} = 7.6 Hz), 7.02 (2H, app. t, ³J_{HH} = 7.5 Hz), 6.86 (2H, app. t, ³J_{HH} = 7.6 Hz), 6.53 (2H, d, ³J_{HH} = 7.6 Hz), 4.50 (4H, m), 1.52 (6H, m) ppm. ¹³C-{¹H} NMR (75 MHz,

CDCl₃) δ_C = 169.6, 166.4, 156.9, 148.7, 147.4, 145.0, 140.2, 138.3, 131.6, 130.4, 130.1, 129.1, 128.1, 127.8, 126.9, 125.5, 125.1, 124.1, 123.5, 120.6, 116.6, 62.2, 14.4 ppm. UV-vis (MeCN): λ_{max} (ε/dm³ mol⁻¹ cm⁻¹) 470 (4500), 350 (22 000), 292 (39 500), 268 (45 650) nm. Elemental analysis: Calcd (%) for C₄₆H₃₆N₄O₄IrPF₆: C, 52.82, H, 3.47, N, 5.36; Found: C, 52.90, H, 3.48, N, 5.36. ES MS found *m/z* 901.3, calculated *m/z* 901.0 for [M – PF₆]⁺. HR MS found *m/z* 901.2370, calculated *m/z* 901.2363 for [C₄₆H₃₆N₄O₄¹⁹¹Ir]⁺. IR (solid): ν 1722 (CO), 837 (PF₆⁻) cm⁻¹.

[Ir(epqc)₂(dmbpy)]PF₆ **3b**. Prepared similarly from **2** (0.069 g, 0.037 mmol) and 4-4'-dimethyl-2,2'-bipyridine (dmbpy) (0.0136 g, 0.074 mmol). Yield = 0.058 g, 85%. ¹H NMR (250 MHz, CDCl₃) δ_H = 8.51 (2H, s), 8.47 (2H, d, ³J_{HH} = 7.9 Hz), 8.01–7.81 (4H, m), 7.72 (2H, d, ³J_{HH} = 7.9 Hz), 7.52–7.31 (4H, m), 7.2–7.0 (4H, m), 6.95 (2H, app. t, ³J_{HH} = 8.5 Hz), 6.83 (2H, app. t, ³J_{HH} = 7.3 Hz), 6.50 (2H, d, ³J_{HH} = 7.3 Hz), 4.62 (4H, q, ³J_{HH} = 7.1 Hz), 2.47 (6H, s), 1.56 (6H, t, ³J_{HH} = 7.2 Hz) ppm. ¹³C-{¹H} NMR (75 MHz, CDCl₃) δ_C = 169.7, 165.2, 155.2, 152.7, 148.9, 146.6, 145.1, 138.7, 134.8, 131.5, 129.8, 129.5, 128.8, 127.6, 127.2, 126.4, 125.3, 123.3, 122.4, 120.2, 118.6, 65.9, 21.3, 15.4 ppm. UV-vis (MeCN): λ_{max} (ε/dm³ mol⁻¹ cm⁻¹) 467 (4200), 350 (23 500), 290 (46 500), 265 (55 300) nm. Elemental analysis: Calcd (%) for C₄₈H₄₀N₄O₄IrPF₆: C, 53.68, H, 3.75, N, 5.22; Found: C, 53.86, H, 3.79, N, 5.26. ES MS found *m/z* 929.3, calculated *m/z* 929.3 for [M – PF₆]⁺. HR MS found *m/z* 927.2650, calculated *m/z* 927.2650 for [C₄₈H₄₀N₄O₄¹⁹¹Ir]⁺. IR (solid): ν 1720 (CO), 829 (PF₆⁻) cm⁻¹.

[Ir(epqc)₂(dmbpc)]PF₆ **3c**. Prepared similarly from **2** (0.069 g, 0.049 mmol) and diethyl-2,2'-bipyridine-4,4'-dicarboxylate (0.028 g, 0.098 mmol). Yield = 0.072 g, 74%. ¹H NMR (250 MHz, CDCl₃) δ_H = 8.67 (2H, d, ³J_{HH} = 7.5 Hz), 8.58 (2H, d, ³J_{HH} = 7.6 Hz), 8.43–8.34 (2H, m), 8.16–8.05 (4H, m), 7.55 (2H, d, ³J_{HH} = 7.5 Hz), 7.45 (2H, app. t, ³J_{HH} = 8.7 Hz), 7.35–7.19 (4H, m), 7.08 (2H, app. t, ³J_{HH} = 8.7 Hz), 6.88 (2H, app. t, ³J_{HH} = 7.6 Hz), 6.51 (2H, d, ³J_{HH} = 7.6 Hz), 4.52 (4H, q, ³J_{HH} = 7.2 Hz), 4.46 (4H, br t), 3.68 (4H, br t), 3.30 (6H, s), 1.48 (6H, t, ³J_{HH} = 7.2 Hz) ppm. ¹³C-{¹H} NMR (75 MHz, CDCl₃) δ_C = 169.6, 166.4, 162.9, 156.7, 150.1, 148.4, 147.1, 144.9, 140.7, 139.0, 134.8, 131.6, 130.0, 129.0, 127.7, 127.1, 124.9, 124.0, 123.2, 120.5, 118.8, 116.6, 70.3, 65.6, 62.9, 61.9, 15.2 ppm. UV-vis (MeCN): λ_{max} (ε/dm³ mol⁻¹ cm⁻¹) 464 (2900), 352 (18 200), 291 (39 500), 267 (47 900) nm. Elemental analysis: Calcd (%) for C₅₄H₄₈N₄O₁₀IrPF₆: C, 51.88, H, 3.87, N, 4.48; Found: C, 51.74, H, 3.84, N, 4.46. ES MS found *m/z* 1105.3, calculated *m/z* 1105.2 for [M – PF₆]⁺. HR MS found *m/z* 1105.2977, calculated *m/z* 1103.2977 for [C₅₄H₄₈N₄O₁₀¹⁹¹Ir]⁺. IR (solid): ν 1724 (CO), 835 (PF₆⁻) cm⁻¹.

[Ir(epqc)₂(phen)]PF₆ **3d**. Prepared similarly from **2** (0.064 g, 0.041 mmol) and 1,10-phenanthroline monohydrate (0.015 g, 0.082 mmol). Yield = 0.060 g, 82%. ¹H NMR (250 MHz, CDCl₃) δ_H = 8.66 (2H, d, ³J_{HH} = 7.6 Hz), 8.52–8.36 (4H, m), 8.23 (2H, d, ³J_{HH} = 7.6 Hz), 8.16 (2H, d, ³J_{HH} = 7.5 Hz), 7.92–7.77 (4H, m), 7.70–7.51 (4H, m), 7.33 (2H, d, ³J_{HH} = 8.2 Hz), 6.90 (2H, app. t, ³J_{HH} = 7.6 Hz), 6.80 (2H, app. t, ³J_{HH} = 7.6 Hz), 6.63 (2H, d, ³J_{HH} = 7.5 Hz), 4.58 (4H, q, ³J_{HH} = 7.3 Hz), 1.53 (6H, t, ³J_{HH} =



7.3 Hz) ppm. $^{13}\text{C}\{-^1\text{H}\}$ NMR (75 MHz, CDCl_3) $\delta_{\text{C}} = 169.6, 164.9, 156.9, 149.6, 148.9, 147.9, 144.6, 138.6, 136.9, 135.0, 130.7, 130.0, 129.7, 128.8, 127.7, 127.4, 126.6, 125.2, 124.3, 123.5, 120.3, 118.6, 62.0, 14.1$ ppm. UV-vis (MeCN): λ_{max} ($\epsilon/\text{dm}^3 \text{mol}^{-1} \text{cm}^{-1}$) 460 (4500), 356 (25 800), 288 (52 800), 269 (65 400) nm. Elemental analysis: Calcd (%) for $\text{C}_{48}\text{H}_{36}\text{N}_4\text{O}_4\text{IrPF}_6$: C, 53.88, H, 3.39, N, 5.24; Found: C, 53.75, H, 3.51, N, 5.28. ES MS found m/z 925.2, calculated m/z 925.2 for $[\text{M} - \text{PF}_6]^+$. HR MS found m/z 923.2345, calculated m/z 923.2337 for $[\text{C}_{48}\text{H}_{36}\text{N}_4\text{O}_4^{191}\text{Ir}]^+$. IR (solid): ν 1722 (CO), 833 (PF_6^-) cm^{-1} .

[Ir(epqc)₂(dip)]PF₆ 3e. Prepared similarly from 2 (0.060 g, 0.037 mmol) and 4,7-diphenyl-1,10-phenanthroline (0.025 g, 0.074 mmol). Yield = 0.060 g, 78%. ^1H NMR (250 MHz, CDCl_3) $\delta_{\text{H}} = 8.61$ (2H, s), 8.51 (2H, d, $^3J_{\text{HH}} = 5.6$ Hz), 8.48 (2H, d, $^3J_{\text{HH}} = 8.2$ Hz), 8.16 (4H, d, $^3J_{\text{HH}} = 7.5$ Hz), 7.81 (2H, s), 7.78 (2H, d, $^3J_{\text{HH}} = 5.6$ Hz), 7.51–7.34 (10H, m), 7.38–7.28 (4H, m), 6.9–6.75 (4H, m), 6.61 (2H, d, $^3J_{\text{HH}} = 7.5$ Hz), 4.60 (4H, q, $^3J_{\text{HH}} = 7.1$ Hz), 1.55 (6H, t, $^3J_{\text{HH}} = 7.1$ Hz) ppm. $^{13}\text{C}\{-^1\text{H}\}$ NMR (75 MHz, CDCl_3) $\delta_{\text{C}} = 170.0, 165.2, 156.7, 151.3, 148.6, 147.2, 145.3, 138.8, 135.2, 131.6, 130.9, 130.1, 129.9, 129.3, 128.7, 128.2, 127.9, 126.9, 126.7, 126.0, 125.6, 124.8, 124.4, 123.8, 120.5, 119.1, 63.0, 14.4$ ppm. UV-vis (MeCN): λ_{max} ($\epsilon/\text{dm}^3 \text{mol}^{-1} \text{cm}^{-1}$) 465 (3600), 344 (23 300), 290 (55 900), 269 (59 000) nm. Elemental analysis: Calcd (%) for $\text{C}_{60}\text{H}_{44}\text{N}_4\text{O}_4\text{IrPF}_6$: C, 58.96, H, 3.63, N, 4.58; Found: C, 58.90, H, 3.57, N, 4.54. ES MS found m/z 1077.3, calculated m/z 1077.2 for $[\text{M} - \text{PF}_6]^+$. HR MS found m/z 1075.2947, calculated m/z 1075.2963 for $[\text{C}_{60}\text{H}_{44}\text{N}_4\text{O}_4^{191}\text{Ir}]^+$. IR (solid): ν 1721 (CO), 835 (PF_6^-) cm^{-1} .

[Ir(epqc)₂(dppz)]PF₆ 3f. Prepared similarly from 2 (0.072 g, 0.046 mmol) and dppz (0.028 g, 0.099 mmol). Yield = 0.081 g, 75%. ^1H NMR (250 MHz, CDCl_3) $\delta_{\text{H}} = 9.46$ (1H, d, $^3J_{\text{HH}} = 8.0$ Hz), 9.39 (1H, d, $^3J_{\text{HH}} = 8.1$ Hz), 9.14 (1H, br s), 8.62–8.55 (2H, m), 8.46 (1H, d, $^3J_{\text{HH}} = 4.8$ Hz), 8.30 (1H, app. t, $^3J_{\text{HH}} = 4.1$ Hz), 8.20–7.90 (4H, m), 7.85 (2H, app. t, $^3J_{\text{HH}} = 6.7$ Hz), 7.80–7.75 (2H, m), 7.71–7.61 (2H, m), 7.49–7.42 (2H, m), 7.30–7.23 (4H, m), 7.16–7.06 (2H, m), 6.80 (2H, app. t, $^3J_{\text{HH}} = 7.7$ Hz), 6.56 (1H, d, $^3J_{\text{HH}} = 7.6$ Hz), 4.46 (4H, q, $^3J_{\text{HH}} = 7.1$ Hz), 1.55 (6H, t, $^3J_{\text{HH}} = 7.1$ Hz) ppm. $^{13}\text{C}\{-^1\text{H}\}$ NMR (75 MHz, CDCl_3) $\delta_{\text{C}} = 169.7, 164.8, 156.3, 152.1, 149.6, 148.7, 148.3, 145.2, 142.8, 138.9, 138.6, 136.0, 135.1, 132.4, 131.5, 130.4, 129.5, 128.6, 127.9, 127.3, 126.8, 124.5, 123.8, 118.9, 62.9, 14.2$ ppm. UV-vis (MeCN): λ_{max} ($\epsilon/\text{dm}^3 \text{mol}^{-1} \text{cm}^{-1}$) 463 (3600), 364 (29 700), 272 (82 600) nm. Elemental analysis: Calcd (%) for $\text{C}_{54}\text{H}_{38}\text{N}_6\text{O}_4\text{IrPF}_6$: C, 55.34, H, 3.27, N, 7.17; Found: C, 55.42, H, 3.33, N, 7.08. ES MS found m/z 1027.3, calculated m/z 1027.3 for $[\text{M} - \text{PF}_6]^+$. HR MS found m/z 1025.2561, calculated m/z 1025.2555 for $[\text{C}_{54}\text{H}_{38}\text{N}_6\text{O}_4^{191}\text{Ir}]^+$. IR (solid): ν 1724 (CO), 830 (PF_6^-) cm^{-1} .

[Ir(epqc)₂(dppn)]PF₆ 3g. Prepared similarly from 2 (0.064 g, 0.041 mmol) and dppn (0.028 g, 0.084 mmol). Yield = 0.078 g, 78%. ^1H NMR (250 MHz, CDCl_3) $\delta_{\text{H}} = 9.43$ (1H, d, $^3J_{\text{HH}} = 8.2$ Hz), 8.92 (1H, br s), 8.76 (1H, s), 8.66 (2H, app. t, $^3J_{\text{HH}} = 4.8$ Hz), 8.55 (1H, d, $^3J_{\text{HH}} = 4.8$ Hz), 8.48–8.41 (2H, m), 8.38–8.31 (2H, m), 8.22 (1H, d, $^3J_{\text{HH}} = 6.7$ Hz), 8.14–8.06 (2H, m), 8.03–7.94 (2H, m), 7.55–7.16 (7H, m), 7.10–6.95 (3H, m), 6.92–6.80 (3H, m), 6.71–6.54 (2H, m), 4.50 (4H, q, $^3J_{\text{HH}} =$

7.1 Hz), 1.48 (6H, t, $^3J_{\text{HH}} = 7.1$ Hz) ppm. $^{13}\text{C}\{-^1\text{H}\}$ NMR (75 MHz, CDCl_3) $\delta_{\text{C}} = 170.2, 165.0, 150.5, 149.8, 148.7, 148.5, 145.2, 138.9, 138.4, 136.5, 136.0, 135.2, 133.7, 131.8, 131.3, 130.0, 129.0, 128.8, 128.2, 128.1, 127.6, 127.1, 126.7, 125.3, 124.7, 124.0, 119.6, 63.0, 14.4$ ppm. UV-vis (MeCN): λ_{max} ($\epsilon/\text{dm}^3 \text{mol}^{-1} \text{cm}^{-1}$) 461 (5400), 416 (12 100), 398 (13 500), 327 (58 600), 292 (51 900), 266 (68 200) nm. Elemental analysis: Calcd (%) for $\text{C}_{58}\text{H}_{40}\text{N}_6\text{O}_4\text{IrPF}_6$: C, 57.00, H, 3.30, N, 6.88; Found: C, 57.01, H, 3.34, N, 6.76. ES MS found m/z 1077.2, calculated m/z 1077.3 for $[\text{M} - \text{PF}_6]^+$. HR MS found m/z 1075.2715, calculated m/z 1075.2711 for $[\text{C}_{58}\text{H}_{40}\text{N}_6\text{O}_4^{191}\text{Ir}]^+$. IR (solid): ν 1719 (CO), 828 (PF_6^-) cm^{-1} .

[Ir(epqc)₂(qdppz)]PF₆ 3h. Prepared similarly from 2 (0.068 g, 0.044 mmol) and qdppz (0.037 g, 0.090 mmol). Yield = 0.094 g, 83%. ^1H NMR (250 MHz, CDCl_3) $\delta_{\text{H}} = 9.38$ (2H, d, $^3J_{\text{HH}} = 5.1$ Hz), 8.64 (2H, s), 8.61 (2H, d, $^3J_{\text{HH}} = 5.0$ Hz), 8.34 (2H, dd, $^3J_{\text{HH}} = 8.6$ and 4.1 Hz), 8.13 (2H, app. t, $^3J_{\text{HH}} = 6.90$ Hz), 8.07–7.92 (3H, m), 7.70 (2H, app. t, $^3J_{\text{HH}} = 8.9$ Hz), 7.56 (1H, d, $^3J_{\text{HH}} = 7.1$ Hz), 7.44 (1H, app. t, $^3J_{\text{HH}} = 7.1$ Hz), 7.38 (2H, app. t, $^3J_{\text{HH}} = 7.9$ Hz), 7.28 (1H, app. t, $^3J_{\text{HH}} = 7.4$ Hz), 7.19 (2H, app. t, $^3J_{\text{HH}} = 7.6$ Hz), 7.15–7.02 (2H, m), 6.94 (2H, app. t, $^3J_{\text{HH}} = 7.5$ Hz), 6.86 (2H, app. t, $^3J_{\text{HH}} = 7.3$ Hz), 6.62 (2H, app. t, $^3J_{\text{HH}} = 5.74$ Hz), 4.50 (4H, q, $^3J_{\text{HH}} = 7.2$ Hz), 1.42 (6H, t, $^3J_{\text{HH}} = 7.2$ Hz) ppm. $^{13}\text{C}\{-^1\text{H}\}$ NMR (75 MHz, CDCl_3) $\delta_{\text{C}} = 166.4, 156.7, 148.9, 138.5, 136.5, 130.2, 130.0, 129.0, 127.9, 127.6, 125.5, 124.1, 120.4, 120.3, 116.5, 62.1, 14.4$ ppm. UV-vis (MeCN): λ_{max} ($\epsilon/\text{dm}^3 \text{mol}^{-1} \text{cm}^{-1}$) 460 (4550), 367 (29 500), 278 (83 750), 212 (85 650) nm. Elemental analysis: Calcd (%) for $\text{C}_{62}\text{H}_{40}\text{N}_6\text{O}_6\text{IrPF}_6$: C, 57.19, H, 3.10, N, 6.45; Found: C, 57.12, H, 3.18, N, 6.40. ES MS found m/z 1157.3, calculated m/z 1157.2 for $[\text{M} - \text{PF}_6]^+$. HR MS found m/z 1155.2587, calculated m/z 1155.2610 for $[\text{C}_{62}\text{H}_{40}\text{N}_6\text{O}_6^{191}\text{Ir}]^+$. IR (solid): ν 1722 (CO), 1610 (CO), 832 (PF_6^-) cm^{-1} .

[Ir(pqca)₂(bpy)]Cl 4a. Complex 3a (0.036 g, 0.020 mmol) was dissolved in acetone (5 ml) and KOH (1 M soln, 5 ml) added. The mixture was stirred at room temp. for 14 h. The solvent was removed *in vacuo* and water (20 ml) added, followed by neutralisation with HCl (1 M soln). Water was removed *in vacuo* and product was dissolved in MeOH (10 ml). The solution was filtered to remove salts and the solvent removed *in vacuo*. Yield = 0.022 g, 65%. ^1H NMR (400 MHz, MeOD) $\delta_{\text{H}} = 8.37$ (2H, s), 8.20–8.15 (4H, m), 8.12 (2H, d, $^3J_{\text{HH}} = 7.7$ Hz), 8.06 (2H, d, $^3J_{\text{HH}} = 7.7$ Hz), 7.89 (2H, app. t, $^3J_{\text{HH}} = 8.0$ Hz), 7.44 (2H, app. t, $^3J_{\text{HH}} = 7.3$ Hz), 7.30 (2H, d, $^3J_{\text{HH}} = 7.6$ Hz), 7.23 (2H, app. t, $^3J_{\text{HH}} = 7.5$ Hz), 7.03 (2H, app. t, $^3J_{\text{HH}} = 7.7$ Hz), 6.87 (2H, app. t, $^3J_{\text{HH}} = 7.7$ Hz), 6.69 (2H, app. t, $^3J_{\text{HH}} = 7.4$ Hz), 6.53 (2H, d, $^3J_{\text{HH}} = 7.7$ Hz) ppm. UV-vis (MeOH): λ_{max} ($\epsilon/\text{dm}^3 \text{mol}^{-1} \text{cm}^{-1}$) 453, (1200), 333 (11 200), 285 (12 350) nm. ES MS found m/z 845.1, calculated m/z 844.9 for $[\text{M} - \text{Cl}]^+$. HR MS found m/z 843.1710, calculated m/z 843.1711 for $[\text{C}_{42}\text{H}_{28}\text{N}_4\text{O}_4^{191}\text{Ir}]^+$. IR (solid): ν 1578 (CO) cm^{-1} .

[Ir(pqca)₂(dmbpy)]Cl 4b. Prepared similarly from 3b (0.050 g, 0.088 mmol). Yield = 0.041 g, 80%. ^1H NMR (250 MHz, MeOD) $\delta_{\text{H}} = 8.67$ (2H, s), 8.70 (2H, d, $^3J_{\text{HH}} = 5.8$ Hz), 8.46 (2H, d, $^3J_{\text{HH}} = 8.2$ Hz), 8.29 (2H, d, $^3J_{\text{HH}} = 8.2$ Hz), 8.19 (2H, d, $^3J_{\text{HH}} = 7.6$ Hz), 7.98 (2H, s), 7.95 (2H, app. t, $^3J_{\text{HH}} =$



6.2 Hz), 7.73 (2H, app. t, $^3J_{\text{HH}} = 7.0$ Hz), 7.44 (2H, d, $^3J_{\text{HH}} = 8.4$ Hz), 7.27 (2H, app. t, $^3J_{\text{HH}} = 7.6$ Hz), 6.82 (2H, app. t, $^3J_{\text{HH}} = 7.1$ Hz), 6.67 (2H, d, $^3J_{\text{HH}} = 7.6$ Hz), 2.57 (6H, s) ppm. $^{13}\text{C}\{-^1\text{H}\}$ NMR (75 MHz, MeOD) $\delta_{\text{C}} = 171.1, 155.5, 1519, 151.2, 147.9, 147.0, 146.2, 134.4, 130.2, 129.6, 129.3, 128.6, 127.6, 127.4, 126.9, 126.2, 125.0, 124.5, 124.3, 122.6, 114.3, 19.8$ ppm. UV-vis (MeOH): λ_{max} ($\epsilon/\text{dm}^3 \text{ mol}^{-1} \text{ cm}^{-1}$) 450 (1600), 341 (6000), 286 (16 800), 267 (18 600) nm. ES MS found m/z 873.2, calculated m/z 873.0 for $[\text{M} - \text{Cl}]^+$. HR MS found m/z 871.2018, calculated m/z 871.2024 for $[\text{C}_{44}\text{H}_{32}\text{N}_4\text{O}_4^{191}\text{Ir}]^+$. IR (solid): ν 1578 (CO) cm^{-1} .

[Ir(pqca)₂(bpdC)]Cl 4c. Prepared similarly from **3c** (0.055 g, 0.053 mmol). Yield = 0.044 g, 91%. ^1H NMR (250 MHz, MeOD) $\delta_{\text{H}} = 8.68$ (2H, br s), 8.38 (2H, s), 8.27 (2H, d, $^3J_{\text{HH}} = 5.7$ Hz), 8.19 (2H, app. t, $^3J_{\text{HH}} = 9.1$ Hz), 7.92 (2H, s), 7.90 (2H, d, $^3J_{\text{HH}} = 5.7$ Hz), 7.43–7.31 (4H, m), 7.17 (2H, app. t, $^3J_{\text{HH}} = 7.7$ Hz), 6.98 (2H, app. t, $^3J_{\text{HH}} = 7.9$ Hz), 6.80 (2H, app. t, $^3J_{\text{HH}} = 7.1$ Hz), 6.53 (2H, d, $^3J_{\text{HH}} = 7.2$ Hz) ppm. $^{13}\text{C}\{-^1\text{H}\}$ NMR (75 MHz, MeOD) $\delta_{\text{C}} = 172.2, 170.4, 160.4, 157.8, 151.0, 150.7, 148.1, 147.2, 146.3, 139.3, 135.4, 134.7, 130.3, 129.9, 129.6, 128.8, 128.6, 127.5, 127.0, 126.7, 126.3, 125.5, 124.4, 122.8, 116.5, 114.5$ ppm. UV-vis (MeOH): λ_{max} ($\epsilon/\text{dm}^3 \text{ mol}^{-1} \text{ cm}^{-1}$) 449 (1300), 338 (5000), 287 (15 700), 262 (20 400) nm. ES MS found m/z 933.1, calculated m/z 932.9 for $[\text{M} - \text{Cl}]^+$. HR MS found m/z 931.1507, calculated m/z 931.1508 for $[\text{C}_{44}\text{H}_{28}\text{N}_4\text{O}_8^{191}\text{Ir}]^+$. IR (solid): ν 1578 (CO) cm^{-1} .

[Ir(pqca)₂(phen)]Cl 4d. Prepared similarly from **3d** (0.040 g, 0.043 mmol). Yield = 0.026 g, 70%. ^1H NMR (400 MHz, MeOD) $\delta_{\text{H}} = 8.81$ (2H, s), 8.62 (2H, d, $^3J_{\text{HH}} = 5.8$ Hz), 8.46 (2H, app. t, $^3J_{\text{HH}} = 8.2$ Hz), 8.29 (2H, d, $^3J_{\text{HH}} = 8.2$ Hz), 8.19 (2H, d, $^3J_{\text{HH}} = 7.6$ Hz), 7.98 (2H, s), 7.95 (2H, app. t, $^3J_{\text{HH}} = 6.2$ Hz), 7.73 (2H, app. t, $^3J_{\text{HH}} = 7.0$ Hz), 7.44 (2H, d, $^3J_{\text{HH}} = 8.4$ Hz), 7.27 (2H, app. t, $^3J_{\text{HH}} = 7.6$ Hz), 6.91 (2H, app. t, $^3J_{\text{HH}} = 7.4$ Hz), 6.82 (2H, app. t, $^3J_{\text{HH}} = 7.1$ Hz), 6.67 (2H, d, $^3J_{\text{HH}} = 7.6$ Hz) ppm. UV-vis (MeOH): λ_{max} ($\epsilon/\text{dm}^3 \text{ mol}^{-1} \text{ cm}^{-1}$) 445 (2600), 339 (11 000), 266 (37 400) nm. ES MS found m/z 869.1, calculated m/z 868.9 for $[\text{M} - \text{Cl}]^+$. HR MS found m/z 867.1704, calculated m/z 867.1711 for $[\text{C}_{44}\text{H}_{28}\text{N}_4\text{O}_4^{191}\text{Ir}]^+$. IR (solid): ν 1597 (CO) cm^{-1} .

[Ir(pqca)₂(dip)]Cl 4e. Prepared similarly from **3e** (0.030 g, 0.024 mmol). Yield 0.018 g, 76%. ^1H NMR (400 MHz, MeOD) $\delta_{\text{H}} = 8.84$ (2H, s), 8.69 (2H, d, $^3J_{\text{HH}} = 7.6$ Hz), 8.53 (2H, d, $^3J_{\text{HH}} = 7.8$ Hz), 8.31 (2H, d, $^3J_{\text{HH}} = 7.6$ Hz), 7.93 (4H, app. t, $^3J_{\text{HH}} = 7.2$ Hz), 7.59–7.49 (12H, m), 7.35 (2H, app. t, $^3J_{\text{HH}} = 6.2$ Hz), 7.28 (2H, app. t, $^3J_{\text{HH}} = 6.8$ Hz), 6.98–6.88 (4H, m), 6.71 (2H, d, $^3J_{\text{HH}} = 7.8$ Hz) ppm. $^{13}\text{C}\{-^1\text{H}\}$ NMR (75 MHz, MeOD) $\delta_{\text{C}} = 172.2, 170.1, 151.0, 150.9, 150.7, 148.1, 147.2, 146.3, 135.4, 134.7, 130.3, 130.0, 129.7, 129.6, 128.8, 128.6, 128.5, 127.5, 127.4, 127.0, 126.7, 126.3, 125.5, 124.4, 122.8, 116.5, 114.5$ ppm. UV-vis (MeOH): λ_{max} ($\epsilon/\text{dm}^3 \text{ mol}^{-1} \text{ cm}^{-1}$) 448 (1700), 402 (1400), 336 (7900), 288 (22 400), 266 (22 600) nm. ES MS found m/z 1021.2, calculated m/z 1021.1 for $[\text{M} - \text{Cl}]^+$. HR MS found m/z 1019.2333, calculated m/z 1019.2337 for $[\text{C}_{56}\text{H}_{36}\text{N}_4\text{O}_4^{191}\text{Ir}]^+$. IR (solid): ν 1576 (CO) cm^{-1} .

[Ir(pqca)₂(dppz)]Cl 4f. Prepared similarly from **3f** (0.052 g, 0.044 mmol). Yield 0.035 g, 79%. ^1H NMR (400 MHz, MeOD) $\delta_{\text{H}} = 9.48$ (2H, d, $^3J_{\text{HH}} = 7.6$ Hz), 8.74 (2H, s), 8.62 (2H, d, $^3J_{\text{HH}} = 5.0$ Hz), 8.38–8.30 (2H, m), 8.22 (2H, d, $^3J_{\text{HH}} = 7.9$ Hz),

8.13–8.05 (3H, m), 7.98 (2H, app. t), 7.87 (2H, br d), 7.75 (1H, app. t), 7.59 (1H, app. t), 7.50–7.40 (3H, m), 7.21–7.12 (2H, m), 6.88–6.80 (2H, m), 6.61 (2H, d, $^3J_{\text{HH}} = 7.6$ Hz) ppm. UV-vis (MeOH): λ_{max} ($\epsilon/\text{dm}^3 \text{ mol}^{-1} \text{ cm}^{-1}$) 435 (1800), 335 (9000), 289 (18 400), 265 (23 400) nm. HR MS found m/z 969.1914, calculated m/z 969.1929 for $[\text{C}_{50}\text{H}_{30}\text{N}_6\text{O}_4^{191}\text{Ir}]^+$. IR (solid): ν 1575 (CO) cm^{-1} .

[Ir(pqca)₂(dppn)]Cl 4g. Prepared similarly from **3g** (0.048 g, 0.039 mmol). Yield 0.029 g, 71%. ^1H NMR (400 MHz, MeOD) $\delta_{\text{H}} = 9.49$ (2H, d, $^3J_{\text{HH}} = 7.6$ Hz), 8.80 (2H, s), 8.61 (2H, dd, $J_{\text{HH}} = 5.3$ and 1.4 Hz), 8.34–8.28 (4H, m), 8.20–7.85 (4H, overlapping m), 7.51–7.38 (5H, m), 7.33 (2H, d, $^3J_{\text{HH}} = 7.6$ Hz), 7.18–7.05 (3H, m), 6.81–6.70 (4H, m), 6.60 (2H, d, $^3J_{\text{HH}} = 7.7$ Hz) ppm. UV-vis (MeOH): λ_{max} ($\epsilon/\text{dm}^3 \text{ mol}^{-1} \text{ cm}^{-1}$) 429 (2600), 330 (17 700), 287 (24 200), 263 (33 800) nm. HR MS found m/z 1019.2089, calculated m/z 1019.2085 for $[\text{C}_{54}\text{H}_{32}\text{N}_6\text{O}_4^{191}\text{Ir}]^+$. IR (solid): ν 1578 (CO) cm^{-1} .

Conclusions

Water-soluble, luminescent iridium(III) complexes can be conveniently synthesised through the use of cinchophen-based ligands. The Ir(III) coordination chemistry of ethyl-2-phenylquinoline-4-carboxylate can be achieved using traditional methods and the resultant cyclometalated complexes are tolerant to the subsequent deprotection strategy. The new complexes of the form $[\text{Ir}(\text{pqca})_2(\text{N}^*\text{N})]^+$ are luminescent *via* an excited state that is best described as possessing substantial $^3\text{MLCT}$ character; the CT nature was reflected in the solvent-sensitive properties of the complexes. TD-DFT calculations also revealed that careful modelling of the protonated form of the carboxylic acid/carboxylate is necessary to allow a more precise approximation of the electronic characteristics of the complexes.

Acknowledgements

We thank Cardiff University and EPSRC for financial support, and the EPSRC National Mass Spectrometry Service Centre at Swansea University.

Notes and references

- (a) R. D. Costa, E. Ortí, H. J. Bolink, F. Monti, G. Accorsi and N. Armaroli, *Angew. Chem., Int. Ed.*, 2012, **51**, 8178; (b) A. F. Rausch, H. H. H. Homeier and H. Yersin, *Top. Organomet. Chem.*, 2010, **29**, 193; (c) N. M. Shavaleev, F. Monti, R. D. Costa, R. Scopelliti, H. J. Bolink, E. Ortí, G. Accorsi, N. Armaroli, E. Baranoff, M. Grätzel and M. K. Nazeeruddin, *Inorg. Chem.*, 2012, **51**, 2263; (d) A. J. Hallett, N. White, W. Wu, X. Cui, P. N. Horton, S. J. Coles, J. Zhao and S. J. A. Pope, *Chem. Commun.*, 2012, **48**, 10838; (e) J. D. Routledge, A. J. Hallett, J. A. Platts, P. N. Horton and S. J. A. Pope, *Eur. J. Inorg. Chem.*, 2012,



- 4065; (f) A. J. Hallett, B. M. Kariuki and S. J. A. Pope, *Dalton Trans.*, 2011, **40**, 9474.
- 2 U. Scherf and D. Neher, *Polyfluorenes*, Springer, Berlin, 2008.
- 3 (a) I.-S. Shin, H.-C. Lim, J.-W. Oh, J.-K. Lee, T. H. Kim and H. Kim, *Electrochem. Commun.*, 2011, **13**, 64; (b) H.-C. Su, Y.-H. Lin, C.-H. Chang, H.-W. Lin, C.-C. Wu, F.-C. Fang, H.-F. Chen and K.-T. Wong, *J. Mater. Chem.*, 2010, **20**, 5521; (c) L. He, L. Duan, J. Qiao, G. Dong, L. Wang and Y. Qiu, *Chem. Mater.*, 2010, **22**, 3535; (d) C. Rothe, C.-J. Chiang, V. Jankus, K. Abdullah, X. Zeng, R. Jitchati, A. S. Batsanov, M. R. Bryce and A. P. Monkman, *Adv. Funct. Mater.*, 2009, **19**, 2038; (e) S. Graber, K. Doyle, M. Neuburger, C. E. Housecroft, E. C. Constable, R. D. Costa, E. Orti, D. Repetto and H. J. Bolink, *J. Am. Chem. Soc.*, 2008, **130**, 14944; (f) R. D. Costa, E. Orti and H. J. Bolink, *Pure Appl. Chem.*, 2011, **83**, 2115.
- 4 (a) E. Baranoff, J.-H. Yum, I. Jung, R. Vulcano, M. Grätzel and Md. K. Nazeeruddin, *Chem.-Asian J.*, 2010, **5**, 496; (b) E. Baranoff, J.-H. Yum, M. Grätzel and Md. K. Nazeeruddin, *J. Organomet. Chem.*, 2009, **694**, 2661.
- 5 (a) V. Fernández-Moreira, F. L. Thorp-Greenwood and M. P. Coogan, *Chem. Commun.*, 2010, **46**, 186; (b) F. L. Thorp-Greenwood, R. G. Balasingham and M. P. Coogan, *J. Organomet. Chem.*, 2012, **714**, 12; (c) K. K.-W. Lo, S. P.-Y. Li and K. Y. Zhang, *New J. Chem.*, 2011, **35**, 265; (d) P.-K. Lee, W. H.-T. Law, H.-W. Liu and K. K.-W. Lo, *Inorg. Chem.*, 2011, **50**, 8570; (e) F. L. Thorp-Greenwood, *Organometallics*, 2012, **31**, 5686.
- 6 (a) B. D. Muegge and M. M. Richter, *Anal. Chem.*, 2004, **76**, 73; (b) J. I. Kim, I.-S. Shin, H. Kim and J.-K. Lee, *J. Am. Chem. Soc.*, 2005, **127**, 1614; (c) M. M. Richter, *Chem. Rev.*, 2004, **104**, 3003; (d) W. Miao, *Chem. Rev.*, 2008, **108**, 2506; (e) F. Kessler, R. D. Costa, D. Di Censo, R. Scopelliti, E. Orti, H. J. Bolink, S. Meier, W. Sarfert, M. Grätzel, Md. K. Nazeeruddin and E. Baranoff, *Dalton Trans.*, 2012, **41**, 180.
- 7 (a) F.-M. Hwang, H.-Y. Chen, P.-S. Chen, C.-S. Liu, Y. Chi, C.-F. Shu, F.-I. Wu, P.-T. Chou, S.-M. Peng and G.-H. Lee, *Inorg. Chem.*, 2005, **44**, 1344; (b) C. Dragonetti, L. Falciola, P. Mussini, S. Righetto, D. Roberto, R. Ugo, A. Valore, F. De Angelis, S. Fantacci, A. Sgamellotti, M. Ramon and M. Muccini, *Inorg. Chem.*, 2007, **46**, 8533; (c) P.-K. Lee, H.-W. Liu, S.-M. Yiu, M.-W. Louie and K. K.-W. Lo, *Dalton Trans.*, 2011, **40**, 2180; (d) E. E. Langdon-Jones, J. D. Routledge, A. J. Hallett, D. Crole, B. D. Ward, J. A. Platts and S. J. A. Pope, *Inorg. Chem.*, 2013, **52**, 448.
- 8 Selected examples (a) W.-H. Zhang, X.-H. Zhang, A. L. Tan, M. A. Yong, D. J. Young and T. S. A. Hor, *Organometallics*, 2012, **31**, 553; (b) K. K.-W. Lo, J. S.-W. Chan, L.-H. Lui and C.-K. Chung, *Organometallics*, 2004, **23**, 3108; (c) R. Tao, J. Qiao, G. Zhang, L. Duan, L. Wang and Y. Qiu, *J. Phys. Chem. C*, 2012, **116**, 11658; (d) W.-J. Xu, S.-J. Liu, T.-C. Ma, Q. Zhao, A. Pertegás, D. Tordera, H. J. Bolink, S.-H. Ye, X.-M. Liu, S. Sun and W. Huang, *J. Mater. Chem.*, 2011, **21**, 13999; (e) C. Dragonetti, A. Valore, A. Colombo, S. Righetto and V. Trifiletti, *Inorg. Chim. Acta*, 2012, **388**, 163; (f) B. Tong, J.-Y. Qiang, Y.-Q. Xu, Q. Mei, T. Duan, Q. Chen and Q.-F. Zhang, *Inorg. Chem. Commun.*, 2011, **14**, 1937; (g) P.-K. Lee, W. H.-T. Law, H.-W. Liu and K. K.-W. Lo, *Inorg. Chem.*, 2011, **50**, 8570; (h) Q. Zhao, F. Li, S. Liu, M. Yu, Z. Liu, T. Yi and C. Huang, *Inorg. Chem.*, 2008, **47**, 9256; (i) K. K.-W. Lo, C.-K. Chung, T. K.-M. Lee, L.-H. Lui, K. H.-K. Tsang and N. Zhu, *Inorg. Chem.*, 2003, **42**, 6886; (j) M.-J. Li, P. Jiao, W. He, C. Yi, C.-W. Li, X. Chen, G.-N. Chen and M. Yang, *Eur. J. Inorg. Chem.*, 2011, 197; (k) M. Schmittel, Q. Shu and M. E. Cinar, *Dalton Trans.*, 2012, **41**, 6064; (l) M.-J. Li, P. Jiao, M. Lin, W. He, G.-N. Chen and X. Chen, *Analyst*, 2011, **136**, 205.
- 9 S. Zanarini, M. Felici, G. Valenti, M. Marcaccio, L. Prodi, S. Bonacchi, P. Contreras-Carballada, R. M. Williams, M. C. Feiters, R. J. M. Noltr, L. De Cola and F. Paolucci, *Chem.-Eur. J.*, 2011, **17**, 4640.
- 10 (a) S. P.-Y. Li, H.-W. Liu, K. Y. Zhang and K. K.-W. Lo, *Chem.-Eur. J.*, 2010, **16**, 8329; (b) H. Yang, L. Li, L. Wan, Z. Zhou and S. Yang, *Inorg. Chem. Commun.*, 2010, **13**, 1387.
- 11 N. B. Sankaran, A. Z. Rys, R. Nassif, M. K. Nayak, K. Metera, B. Chen, H. S. Bazzi and H. F. Sleiman, *Macromolecules*, 2010, **43**, 5530.
- 12 (a) W. Jiang, Y. Gao, Y. Sun, F. Ding, Y. Xu, Z. Bian, F. Li, J. Bian and C. Huang, *Inorg. Chem.*, 2010, **49**, 3252; (b) C. Li, J. Lin, Y. Guo and S. Zhang, *Chem. Commun.*, 2011, **47**, 4442.
- 13 N. D. McDaniel, F. J. Coughlin, L. L. Tinker and S. Bernhard, *J. Am. Chem. Soc.*, 2008, **130**, 210.
- 14 (a) A. Habibagahi, Y. Mébarki, Y. Sultan, G. A. Yap and R. J. Crutchley, *ACS Appl. Mater. Interfaces*, 2009, **1**, 1785; (b) K. K.-W. Lo, C.-K. Chung and N. Zhu, *Chem.-Eur. J.*, 2003, **9**, 475; (c) K. Konishi, H. Yamaguchi and A. Harada, *Chem. Lett.*, 2006, 720.
- 15 (a) J. P. Michael, *Nat. Prod. Rep.*, 1997, **14**, 605; (b) M. Balasubramanian and J. G. Keay, in *Comprehensive Heterocyclic Chemistry II*, ed. A. R. Katritzky, C. W. Rees and E. F. V. Scriven, Pergamon Press, Oxford, New York, 1996, vol. 5, p. 245; (c) A. Burger, *Medicinal Chemistry*, Interscience, New York, NY, 2nd edn, 1960, p. 349; (d) J. C. Krantz and C. J. Carr, *The Pharmacological Principle of Medical Practice*, Williams and Wilkins, Baltimore, MD, London, 6th edn, 1965, p. 826.
- 16 (a) R. D. Larsen, E. G. Corley, A. O. King, J. D. Carrol, P. Davis, T. R. Verhoeven, P. J. Reider, M. Labelle, J. Y. Gauthier, Y. B. Xiang and R. J. Zamboni, *J. Org. Chem.*, 1996, **61**, 3398; (b) Y.-L. Chen, K.-C. Fang, J.-Y. Sheu, S.-L. Hsu and C.-C. Tzeng, *J. Med. Chem.*, 2001, **44**, 2374; (c) G. Roma, M. D. Braccio, G. Grossi, F. Mattioli and M. Ghia, *Eur. J. Med. Chem.*, 2000, **35**, 1021; (d) D. Dubé, M. Blouin, C. Brideau, C.-C. Chan, S. Desmarais, D. Ethier, J.-P. Falgoutyret, R. W. Friesen, M. Girard, Y. Girard, J. Guay, D. Riendeau, P. Tagari and R. N. Young, *Bioorg. Med. Chem. Lett.*, 1998, **8**, 1255; (e) M. P. Maguire, K. R. Sheets, K. McVety, A. P. Spada and A. Zilberstein, *J. Med. Chem.*,



- 1994, **37**, 2129; (f) S.-Y. Tanaka, M. Yasuda and A. Baba, *J. Org. Chem.*, 2006, **71**, 800.
- 17 P. W. Baures, S. A. Peterson and J. W. Kelly, *Bioorg. Med. Chem.*, 1998, **6**, 1389.
- 18 S. Vilar, L. Santana and E. Uriarte, *J. Med. Chem.*, 2006, **49**, 1118.
- 19 M. Nonoyama, *Bull. Chem. Soc. Jpn.*, 1974, **47**, 767.
- 20 K. Y. Zhang, S. P.-Y. Li, N. Zhu, I. W.-S. Or, M. S.-H. Cheung, Y.-W. Lam and K. K.-W. Lo, *Inorg. Chem.*, 2010, **49**, 2530.
- 21 H.-Y. Chen, C.-H. Yang, Y. Chi, Y.-M. Cheng, Y.-S. Yeh, P.-T. Chou, H.-Y. Hsieh, C.-S. Liu, S.-M. Peng and G.-H. Lee, *Can. J. Chem.*, 2006, **84**, 309.
- 22 (a) F. Neve, A. Crispini, S. Campagna and S. Serroni, *Inorg. Chem.*, 1999, **38**, 2250; (b) S. Ladouceur, D. Fortin and E. Zysman-Colman, *Inorg. Chem.*, 2010, **49**, 5625.
- 23 (a) A. Mishra, P. K. Nayak, D. Ray, M. P. Patankar, K. L. Narasimhan and N. Periasamy, *Tetrahedron Lett.*, 2006, **47**, 4715; (b) B. W. D. Andrade, S. Datta, S. R. Forrest, P. Djurovich, E. Polikarpov and M. E. Thompson, *Org. Electron.*, 2005, **6**, 11.
- 24 J. E. Jones, R. L. Jenkins, R. S. Hicks, A. J. Hallett and S. J. A. Pope, *Dalton Trans.*, 2012, **41**, 10372.
- 25 K. K.-K. Lo, C.-K. Chung and N. Zhu, *Chem.-Eur. J.*, 2006, **12**, 1500.
- 26 A referee is thanked for stimulating and guiding comments.
- 27 N. G. Connelly and W. E. Geiger, *Chem. Rev.*, 1996, **96**, 877.
- 28 *SHELXL-PC Package*, Bruker Analytical X-ray Systems, Madison, WI, 1988.
- 29 M. J. Frisch, G. W. Trucks, H. B. Schlegel, G. E. Scuseria, M. A. Robb, J. R. Cheeseman, J. A. Montgomery Jr., T. Vreven, K. N. Kudin, J. C. Burant, J. M. Millam, S. S. Iyengar, J. Tomasi, V. Barone, B. Mennucci, M. Cossi, G. Scalmani, N. Rega, G. A. Petersson, H. Nakatsuji, M. Hada, M. Ehara, K. Toyota, R. Fukuda, J. Hasegawa, M. Ishida, T. Nakajima, Y. Honda, O. Kitao, H. Nakai, M. Klene, X. Li, J. E. Knox, H. P. Hratchian, J. B. Cross, V. Bakken, C. Adamo, J. Jaramillo, R. Gomperts, R. E. Stratmann, O. Yazyev, A. J. Austin, R. Cammi, C. Pomelli, J. W. Ochterski, P. Y. Ayala, K. Morokuma, G. A. Voth, P. Salvador, J. J. Dannenberg, V. G. Zakrzewski, S. Dapprich, A. D. Daniels, M. C. Strain, O. Farkas, D. K. Malick, A. D. Rabuck, K. Raghavachari, J. B. Foresman, J. V. Ortiz, Q. Cui, A. G. Baboul, S. Clifford, J. Cioslowski, B. B. Stefanov, G. Liu, A. Liashenko, P. Piskorz, I. Komaromi, R. L. Martin, D. J. Fox, T. Keith, M. A. Al-Laham, C. Y. Peng, A. Nanayakkara, M. Challacombe, P. M. W. Gill, B. Johnson, W. Chen, M. W. Wong, C. Gonzalez and J. A. Pople, *Gaussian 03, Revision E.01*, Gaussian, Inc., Wallingford, CT, 2004.
- 30 (a) P. J. Hay and W. R. Wadt, *J. Chem. Phys.*, 1985, **82**, 270; (b) P. J. Hay and W. R. Wadt, *J. Chem. Phys.*, 1985, **82**, 299.
- 31 (a) M. M. Francl, W. J. Pietro, W. J. Hehre, J. S. Binkley, D. J. DeFrees, J. A. Pople and M. S. Gordon, *J. Chem. Phys.*, 1982, **77**, 3654; (b) P. C. Hariharan and J. A. Pople, *Theor. Chem. Acc.*, 1973, **28**, 213.
- 32 R. Ditchfield, W. J. Hehre and J. A. Pople, *J. Chem. Phys.*, 1971, **54**, 724.
- 33 M. J. Frisch, G. W. Trucks, H. B. Schlegel, G. E. Scuseria, M. A. Robb, J. R. Cheeseman, G. Scalmani, V. Barone, B. Mennucci, G. A. Petersson, H. Nakatsuji, M. Caricato, X. Li, H. P. Hratchian, A. F. Izmaylov, J. Bloino, G. Zheng, J. L. Sonnenberg, M. Hada, M. Ehara, K. Toyota, R. Fukuda, J. Hasegawa, M. Ishida, T. Nakajima, Y. Honda, O. Kitao, H. Nakai, T. Vreven, J. A. Montgomery Jr., J. E. Peralta, F. Ogliaro, M. Bearpark, J. J. Heyd, E. Brothers, K. N. Kudin, V. N. Staroverov, T. Keith, R. Kobayashi, J. Normand, K. Raghavachari, A. Rendell, J. C. Burant, S. S. Iyengar, J. Tomasi, M. Cossi, N. Rega, J. M. Millam, M. Klene, J. E. Knox, J. B. Cross, V. Bakken, C. Adamo, J. Jaramillo, R. Gomperts, R. E. Stratmann, O. Yazyev, A. J. Austin, R. Cammi, C. Pomelli, J. W. Ochterski, R. L. Martin, K. Morokuma, V. G. Zakrzewski, G. A. Voth, P. Salvador, J. J. Dannenberg, S. Dapprich, A. D. Daniels, O. Farkas, J. B. Foresman, J. V. Ortiz, J. Cioslowski and D. J. Fox, *GAUSSIAN 09 (Revision C.01)*, Gaussian, Inc., Wallingford, CT, 2010.
- 34 J. Tomasi, B. Mennucci and R. Cammi, *Chem. Rev.*, 2005, **105**, 2999 and references therein.
- 35 L. Monti and G. Franchi, *Gazz. Chim. Ital.*, 1951, **81**, 544.
- 36 C. M. Dupureur and J. K. Barton, *Inorg. Chem.*, 1997, **36**, 33.
- 37 (a) V. W. W. Yam, K. K. W. Lo, K. K. Cheung and R. Y. C. Kong, *J. Chem. Soc., Chem. Commun.*, 1995, 1191; (b) M. Shilpa, P. Nagababu, Y. P. Kumar, J. N. L. Latha, M. R. Reddy, K. S. Karthikeyan, N. Md. Gabra and S. Satyanarayana, *J. Fluoresc.*, 2011, **21**, 1155.
- 38 (a) R. López, B. Loeb, T. Boussie and T. J. Meyer, *Tetrahedron Lett.*, 1996, **37**, 5437; (b) A. Ambroise and B. G. Maiya, *Inorg. Chem.*, 2000, **39**, 4256.

